SSRG International Journal of Electrical and Electronics Engineering
ISSN: 2348-8379/ https://doi.org/10.14445/23488379/IJEEE-V11I11P116

Volume 11 Issue 11, 150-159, November 2024

Original Article

Optimized Squared Cosine Pulse Shaping of GFDM with Improved Hippopotamus Optimization for 5G and Beyond Applications

Deepak Kumar Ray[1], Shruti Oza[2]

[1,2]*Department of Electronics and Telecommunication, Bharati Vidyapeeth Deemed to be University College of Engineering, Maharashtra, India.*

[1]*Corresponding Author : dkray@bvucoep.edu.in*

Received: 09 September 2024 Revised: 10 October 2024 Accepted: 08 November 2024 Published: 30 November 2024

Abstract - *Generalized Frequency Division Multiplexing (GFDM) is a cutting-edge multiplexing technique that promises high-speed, low-latency, and reliable 5G communications. Nevertheless, GFDM signals often suffer from excessive Out-of-Band Emissions (OBE), causing interference to other users. This research proposes a novel approach combining pulse shaping and wavelet transformation to mitigate these issues. Specifically, Squared Cosine Pulse Shape Filtering (SCos-PSF) is employed to filter out unwanted interference from the GFDM signal. To optimize the roll-off factor in SCos-PSF, an Improved Hippopotamus Optimization (ImHO) algorithm is introduced. This method is implemented in MATLAB, and its performance is evaluated using metrics such as Bit Error Rate (BER), Peak to Average Power Ratio (PAPR), and Complementary Cumulative Distribution Function (CCDF). The experimental results demonstrate a significant reduction in BER at a Signal-to-Noise Ratio (SNR) of* $1.58*10^{-6}$ *50 dB, showcasing the effectiveness of the proposed approach.*

Keywords - *Generalized Frequency Division Multiplexing, Fifth generation, Bit error rate reduction, Quadrature Enhanced Spatial Modulation, Squared cosine pulse shaping, Improved Hippopotamus Optimization algorithm*

1. Introduction

Recently, Fifth-Generation (5G) and beyond-5G Wireless Communication (WC) systems have significantly enhanced the user experience by offering higher data rates and more efficient multicarrier modulation [1]. While the 4G system utilizes Orthogonal Frequency Division Multiplexing (OFDM), which provides broader Bandwidth (BW) and improved synchronization [2, 3], it suffers from drawbacks such as high Peak-to-Average Power Ratio (PAPR), bandwidth loss, and Increased Out-of-Band EMISSIONS (IOOB) due to orthogonal errors [4, 5]. As future wireless systems demand lower power consumption and reduced latency [6], OFDM becomes insufficient.

To address these limitations, Multicarrier Non-orthogonal Waveforms (MNW) have emerged, with Filter Bank Multicarrier (FBMC) and Generalized Frequency Division Multiplexing (GFDM) as two prominent examples [7]. While FBMC eliminates the need for a Cyclic Prefix (CP), improving Spectral Efficiency (SE) and preventing data fading [8], it requires numerous filters due to early signal fading [9]. In contrast, GFDM, a block-based multicarrier waveform that leverages pulse shaping filters to enhance subcarriers and sub-symbols [12], offers advantages such as low PAPR, high SE, and reduced IOOB due to minimal CP usage. However, its lack of orthogonality increases computational complexity [13-15].

Numerous studies have explored the application of GFDM in various domains, including MIMO systems [16], cognitive radio networks [17], optical communications [18], and filter designs [19]. However, integrating GFDM with modern services can lead to significant self-interference and cross-interference, resulting in high-frequency impairments like imbalanced in-phase/quadrature components and increased Carrier Frequency Offset (CFO) [20]. Strategies such as interference avoidance, CP elimination, and pulse smoothing techniques are essential to mitigate these challenges.

In wireless communication, metaheuristic algorithms like Hippopotamus Optimization (HO) are valuable for optimizing signal processing, resource allocation, and network parameters. These tasks often require an effective trade-off between stability and flexibility to accommodate high-dimensional, nonlinear parameters an area where the HO has shown promise [10].

This study introduces a novel pulse-shaping technique, combined with an Improved Hippopotamus Optimization algorithm, to enhance the performance of the GFDM system. By adopting GFDM systems, higher data rates and lower latency can be achieved, and multicarrier modulation for a wider range of wireless communication applications can be supported.

1.1. Motivation

The increasing demand for high-speed, low-latency communication has led to the development of GFDM-MIMO systems. These systems are essential for various applications, including wireless networks, IoT, smart grids, and vehicular communication, where robust and efficient data transmission is crucial.

While existing methods for enhancing GFDM-MIMO performance face challenges such as bandwidth loss, high computational complexity, interference, and high Bit Error Rate (BER), this research proposes a novel Squared Cosine Pulse Shape Filtering (SCos-PSF) technique to mitigate these issues. By evaluating the performance of the proposed GFDM system under different scenarios, the research demonstrates significant improvements over traditional GFDM systems.

Ultimately, this research aims to address the limitations of existing GFDM-MIMO systems and provide a more efficient and reliable communication solution for 5G and future wireless technologies. The rest of the sections are organized as follows: Section 2 presents the literature survey of the recently published paper. Section 3 demonstrates a detailed description of the proposed QESM-GFDM system. Section 4 evaluates the results and discussion. Section 5 explains the conclusion of the proposed technique.

2. Related works

Using enhanced modulation, Kumar and Prasad [21] evaluated GFDM's performance for 5G wireless applications. Their LCP-GFDM-IQIM technique improved diversity by splitting user data symbols and mapping quadrature/in-phase components using the interleaved quadrature technique. Experiments achieved 30 bpHz EE at 20 Hz, but the GFDM system suffered from increased interference with more users. Wang et al. [22] developed CFO evaluation techniques for GFDM systems, including integral and fractional CFO methods, to identify signal degradation caused by noise and interference. A music algorithm was implemented to enhance GFDM performance, achieving an MSE of less than 0.002. However, the algorithm's effectiveness diminished in 5G and beyond applications. Kumar et al. [23] analyzed PAPR in GFDM systems for 5G, introducing DCT and DST pre-coding and clipping/companding to reduce interference. Experimental results showed a 2-4 dB SNR improvement and a 0.0001 BER. However, clipping led to information loss and increased error rates. Tasadduq et al. [24] proposed CPM to enhance GFDM performance, replacing conventional mapping and de-mapping. Experimental analysis evaluated BER, delay, and power consumption. However, integrating CPM into GFDM was complex and costly. Gupta and Gamad [25] introduced RRC filtering to improve GFDM performance, smoothing symbols within subcarriers. Using AWGN and ZF channels, they analyzed SER performance, achieving 0.001 SER. However, the system's inflexibility and data loss limited its suitability for modern 5G applications.

Metaheuristic algorithms like Hippopotamus Optimization (HO) are valuable in wireless communication for optimizing signal processing, resource allocation, and network parameters. HO's ability to balance stability and flexibility makes it suitable for high-dimensional, nonlinear problems [26]. [27] Heidari et al. further improved convergence speed and expanded its application to complex, multi-dimensional problems. Researchers introduced ImHO, which integrates additional sampling and crossover techniques. These modifications enhance global search capabilities and optimize initial population diversity, which is crucial for multi-objective optimization in wireless networks [28].

2.1. Problem Statement

Current GFDM systems suffer from interference and high latency, limiting their performance. Achieving high data rates and low latency is crucial for future 5G applications in MIMO, IoT, cognitive radio, and optical communication systems. While recent studies introduced novel techniques, challenges like high latency, computational complexity, and low reliability persist. This research proposes a novel approach combining pulse shaping with an improved hippopotamus optimization algorithm to improve GFDM performance, addressing communication complexities.

3. Proposed Methodology

Modern wireless systems demand high capacity, speed, reliability, and low latency for 5G and beyond applications. Traditional OFDM suffers from spectrum loss, increasing bit error rates. GFDM offers improved efficiency and reduced interference, but performance declines due to poor pulse shaping and increased interference in 5G environments. This study proposes SCos-PSF to filter subcarriers without interference, combined with an Improved Hippopotamus Optimization algorithm (ImHO) to improve modulation performance and reduce error rates in the GFDM system. The proposed GFDM system's performance is evaluated using AWGN channels across various metrics.

3.1. System Model

GFDM blocks map and modulate the data onto subcarriers centered at the frequency of $\exp(-2\pi km/M)$ Figure 1 shows.

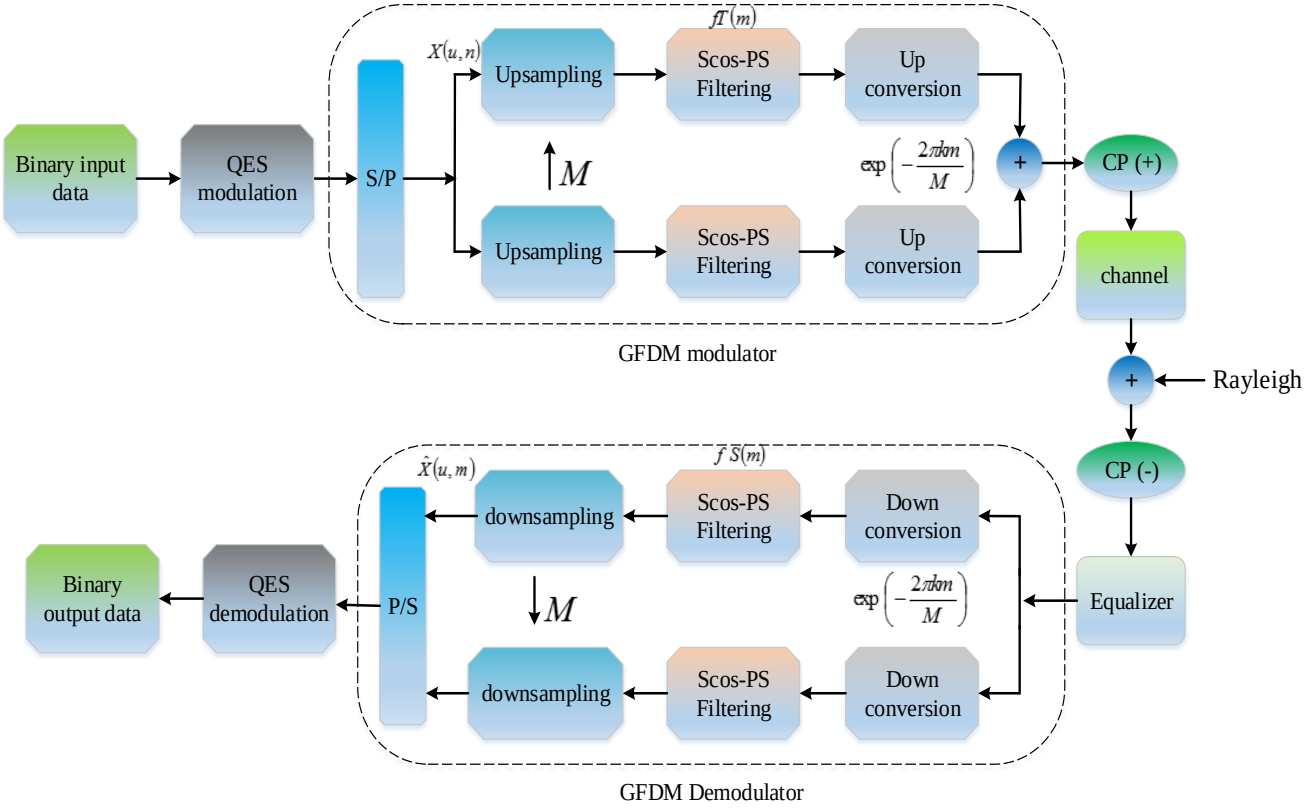

Fig. 1 Transceiver block of the GFDM system

GFDM system's transceiver block diagram. The GFDM transmitter receives random binary input data and modulates it using I/Q mapping. To meet the Nyquist criterion, each symbol is sampled with range M that provides the vector NM efficiently. Pulse Shape Filtering (PSF) ensures the periodicity of NxM and shape subcarriers, improving BER performance. GFDM modulates blocks containing sub-carriers and sub-symbols.

This study employs SCos-PSF to filter sub-carriers in both time and frequency domains, aiding in split and dynamic spectrum allocation by minimizing interference and unwanted out-of-band emissions. After placing the data symbols X(u,n) column-wise, all the symbols are added to form the GFDM signal. In the communication system X9u,n) consist of intricate data symbols, sub-symbols k and subcarriers u. The concatenation of the columns forms the matrix d, and it is depicted below:

$$X = \begin{bmatrix} X(0,0) & \cdots & X(0,N-1) \\ \vdots & \ddots & \vdots \\ X(U-1) & \cdots & X(U-1,N-1) \end{bmatrix} \quad (1)$$

The UxK matrix is considered as a data block where, u=0….U-1are the subcarriers and k=0….K-1 are the time slot elements. The transmission signal can be mathematically formulated as follows,

$$y(m) = \sum_{u=0}^{U-1}\sum_{n=0}^{N-1} X(u,n)[fT(m-uM) mod M\ N] \exp\left(-\frac{2\pi um}{M}\right), 0 \le m \le MN-1 \quad (2)$$

Here u, it represents subcarriers, m represents GFDM samples, represents the total GFDM samples, N represents the total sub-symbols, and T represents the time period. The generated GFDM signal is corrupted by a Frequency-Selective (FS) Rayleigh channel. The obtained time samples z(m), followed by data equalization, are processed at the receiver. The final received signal m=nM can be mathematically expressed as follows:

$$\hat{X}(u,n) = \left(z(m)\exp\left(-\frac{2\pi um}{M}\right)\right) \otimes fS(m)|_{m=NM} \quad (3)$$

Here, X̂(u,m) they are generated by reversing the frequency shift and applying down sampling and matched filter fS(m), ⊗ representing the circular convolution. At last, the receiver computes the invert operation to recover the GFDM signal effectively.

3.2. Pulse Shape Filtering Using SCos-PSF

In this study, the GFDM modulator utilizes the squared cosine PSF (SCos-PSF) technique to filter the GFDM signal using the roll-off factor β. The mathematical formulation of the Cos-PSF is depicted below:

$$f_{Cos}(t)=\begin{Bmatrix} 1 & |t|\le\frac{(1-\beta)T}{2} \\ \frac{1}{2}\left[1+\cos\left(A_{SCos}(t)\right)\right], & \frac{(1-\beta)T}{2}<|t|\le\frac{(1+\beta)T}{2} \\ 0 & otherwise \end{Bmatrix} \quad (4)$$

Here, $A_{SCos}(t)$ represents the cosine arguments and it is mathematically formulated as,

$$A_{SCos}(t)=\frac{|t|-\frac{(1-\beta)T}{2}}{\beta T} \quad (5)$$

The cosine arguments are then modified using a novel Meyer-based orthogonal auxiliary function η, and it can be mathematically formulated as,

$$A_{SCos}(t)=\eta\left(\frac{|t|-\frac{(1-\beta)T}{2}}{\beta T}\right) \quad (6)$$

Finally, the squared cosine PSF can be represented as,

$$F_{Cos}(t)=\sqrt{f_{Cos}(t)} \quad (7)$$

The filtered signal is fed into the Rayleigh channel and finally reaches the receiver end. The distorted data are restored using the proper channel equalization technique and fed into the GFDM demodulator unit, and the obtained signal can be mathematically formulated as follows,

$$\lambda^{r}_{LWT}[m]=\sum_{m=0}^{U-1}v[m]2^{\frac{i}{2}}\mu\left(2^{i}m-r\right),\ i=0,1,2,....,U-1,\ r=0,1,2,.....,U-1 \quad (8)$$

Here, v[m] indicates the time domain data. Here, the optimal best roll-off factor β, is chosen using the novel Improved Hippopotamus Optimization (ImHO) algorithm for enhancing the performance of the PSF. The roll-off factor plays a significant role in pulse shaping. The higher roll-off factor reduces ISI but consumes more bandwidth, causing spectral inefficiencies. In contrast, the lower roll-off factor provides a narrower bandwidth but introduces higher interference. Thus, to overcome the issue, in the proposed pulse shaping, the optimal roll-off factor is chosen using ImHO by considering fitness factors like BER and SNR.

3.2.1. Mathematical Modeling of the ImHO Algorithm

The proposed ImHO algorithm for the optimal best roll-off factor identification is designed by adding iterative mapping in the conventional hippopotamus optimization algorithm to enhance the convergence rate in acquiring the best global solution. The search agents are in the search area arbitrarily and are signified as:

$$D_m: d_{m,r}=G_r+k\cdot\left(H_r-G_r\right),\qquad m=1,2,..P;\ r=1,2,...E \quad (9)$$

Here, the total search agent is defined as P k signifies the arbitrary factor between 0 and 1 and r specifies the dimension. H_r and G_r are the bounds of the solution and D_m is the solution arrived by the m^{th} search agent, and the solution arrived by the m^{th} search agent with r^{th} decision variable is defined as $d_{m,r}$. The search agents are localized in matrix format and are represented as:

$$D=\begin{bmatrix} D_1 \\ \vdots \\ D_m \\ \vdots \\ D_P \end{bmatrix}_{P\times E}=\begin{bmatrix} d_{1,1} & \cdots & d_{1,r} & \cdots & d_{1,E} \\ \vdots & \ddots & \vdots & \iddots & \vdots \\ d_{m,1} & \cdots & d_{m,r} & \cdots & d_{m,E} \\ \vdots & \iddots & \vdots & \ddots & \vdots \\ d_{P,1} & \cdots & d_{P,r} & \cdots & d_{P,r} \end{bmatrix}_{P\times E} \quad (10)$$

3.2.2. Exploration

The solution updated by the search agent in the exploration phase by considering the group behavior of the hippo is expressed as:

$$D^{X}_{m}: d^{X}_{m,r}=d_{m,r}+y1\cdot\left(R-N_1 d_{m,r}\right)\ \ m=1,2,...\frac{P}{2}\ and\ r=1,2,..E \quad (11)$$

Here, the dominant search agent is denoted as R, and the male members in the group are denoted as X. y1 signifies the arbitrary parameter with the bounds [0,1], and N1 is the parameter with an assigned value 1 or 2. The iterative mapping is added in this phase for elevating the convergence rate, which is expressed as:

$$D_{l+1}=abs\left(\sin\left(\frac{I}{D_l}\right)\right) \quad (12)$$

Here, the position updating by the ImHO algorithm based on the iterative map is signified as D_{l+1}, and the same in the past iteration is notated as D_l. The control factor is signified as I that is bounded in [0,1], and the solution obtained by the hippo search agent is formulated as:

$$D^{X}_{m}: d^{X}_{m,r}=0.5\left[abs\left(\sin\left(\frac{I}{D_l}\right)\right)\right]+0.5\left[d_{m,r}+y1\cdot\left(R-N_1 d_{m,r}\right)\right] \quad (13)$$

Here, the iterative mapping makes the algorithm search over more areas and assists in solving the local solution trapping. Besides, the control parameter enhances the convergence rate by avoiding the solution away from the required solution. After updating the male search agents, the female and other imperfect search agents update the solution based on:

$$d_{m,r}^{Y}=\begin{cases} d_{m,r}+e_1\cdot R-N_2\cdot EB_m & if\ M>0.6 \\ d_{r,m}+W_2\cdot EB_m-R & if\ k_6>0.5 \\ G_r+k_7\cdot\left(H_r-G_r\right) & otherwise \end{cases} \quad (14)$$

Here, arbitrary parameters are denoted as e_1 and W_2, the average of the solution is notated as EB_m, condition check is done based on M and arbitrary parameters are denoted as k_6 and k_7. The fitness is formulated based on the following:

$$d_m=\begin{cases} d_m^X, & if\ Fit\left(d_m^X\right)<Fit\left(d_m\right) \\ d_m, & Otherwise \end{cases} \quad (15)$$

Here, $Fit(\cdot)$ signifies the fitness factor.

3.2.3. Exploration-2

The position updating by the hippo search agents in the exploration phase-2 is devised based on the aggressive behavior of the hippo. In this, the hippo makes a louder voice towards the predator when the predator is closer; the movement towards the predator is limited. The solution accomplished by the Exploration phase-2 is formulated as:

$$D_m^Z:d_{m,r}^Z=\begin{cases} \vec{J}\oplus U_r+\left(\frac{z}{\lambda\times cos(2\pi b)}\right)\cdot\left(\frac{1}{\vec{S}}\right)F & it_{U_r}<Fit_m \\ \vec{J}\oplus U_r+\left(\frac{z}{\lambda\times cos(2\pi b)}\right)\cdot\left(\frac{1}{2\times\vec{S}+\vec{k_9}}\right)F & it_{U_r}<Fit_m \end{cases} \quad (16)$$

Here, U signifies the predator, $\vec{J}$ denotes the levy flight and D^Z_m notates the solution of the search agent while detecting the extruder. $\vec{k_9}$ signifies the arbitrary parameter bounds in[1xE], b bounds in [-1,1], and z bounds among 4 and 2. The aggregating movement of the hippo search agent is denoted asλ and $\vec{S}$ is the arbitrary parameter with bounds [2,3]. The fitness is formulated based on the following:

$$D_m=\begin{cases} D_m^Z, & Fit_m^Z<Fit_m \\ D_m & Fit_m^Z\geq Fit_m \end{cases} \quad (17)$$

3.2.4. Exploitation

In the exploitation phase, the hippo search agents are moved to the protected area, and the updating is devised as:

$$D_m^V:d_{m,r}^V=d_{m,r}+k_{10}\cdot\left(G_r^{lo}+g1\cdot\left(H_r^{lo}-G_r^{lo}\right)\right) \quad (18)$$

Here, the protected area is signified as D^V_m the required area z for hiding is denoted as g1 and the required area for hiding is identified based on:

$$g=\begin{cases} 2\times\overrightarrow{k_{11}}-1 \\ k_{12} \\ k_{13} \end{cases} \quad (19)$$

Here, k_{12} and k_{13} signifies the arbitrary parameter and random variable $\overrightarrow{k_{11}}$ then, the fitness is formulated based on:

$$D_m=\begin{cases} D_m^V, & Fit_m^V<Fit_m \\ D_m & Fit_m^V\geq Fit_m \end{cases} \quad (20)$$

3.2.5. Termination

The accomplishment of the optimal best roll-off factor or the completion of iteration terminates the processing of the ImHO algorithm. The pseudo-code is presented in Algorithm 1.

Algorithm 1: Pseudo-code for ImHO algorithm

Pseudo-Code for ImHO Algorithm	
1	The parameters like population and iterations are defined
2	Output: Optimal best roll-off factor
3	For *l*:1:L
4	Feasibility evaluation based on BER and SNR
5	Stage 1: Exploration-1
6	For m=1:P/2
7	Solution updating based on $D_m^X.d_{m,r}^X=0.5\left[abs\left(sin\left(\frac{I}{D_l}\right)\right)\right]+0.5\left[d_{m,r}+y1\cdot\left(R-N_1d_{m,r}\right)\right]$
8	Fitness evaluation based on $d_m=\begin{cases} d_m^X, i & fFit(d_m^X)<Fit(d_m) \\ d_m, & Otherwise \end{cases}$
9	End for
10	Stage 2: Exploration-2
11	For
12	Solution updating based on $D_m^Z:d_{m,r}^Z=\begin{cases} \vec{J}\oplus U_r+\left(\frac{z}{\lambda\times\cos(2\pi b)}\right)\cdot\left(\frac{1}{\vec{S}}\right) & Fit_{U_r}<Fit_m \\ \vec{J}\oplus U_r+\left(\frac{z}{\lambda\times\cos(2\pi b)}\right)\cdot\left(\frac{1}{2\times\vec{S}+\vec{k_9}}\right) & Fit_{U_r}<Fit_m \end{cases}$
13	Fitness evaluation based on $D_m=\begin{cases} D_m^Z, & Fit_m^Z<Fit_m \\ D_m & Fit_m^Z\geq Fit_m \end{cases}$

14	End for
15	Stage 3: Exploitation
16	For
17	Solution updating based on $D_m^V : d_{m,r}^V = d_{m,r} + k_{10} \cdot \left(G_r^{lo} + g1 \cdot \left(H_r^{lo} - G_r^{lo}\right)\right)$
18	Fitness evaluation based on $D_m = \begin{cases} D_m^V, & Fit_m^V < Fit_m \\ D_m & Fit_m^V \geq Fit_m \end{cases}$
19	End for
20	Return the best solution.
21	End

Here, the pulse shaping is employed to obtain enhanced performance using the optimal best roll-off factor. Finally, different performances like BER, CCDF, and PAPR are performed to verify whether the obtained signal is the same as the signal sent by the transmitter.

4. Results and Discussion

The proposed method was realized on the MATLAB platform. Key performance indicators, including Bit Error Rate (BER), Peak-to-average Power Ratio (PAPR), and Complementary Cumulative Distribution Function (CCDF), were evaluated and benchmarked against existing methods. Omitting the receiver's Cyclic Prefix (CP) during simulation enhanced system performance. Table 1 summarizes the simulation parameters for the proposed system.

Table 1. Simulation parameters of the proposed system

Parameters	Values
GFDM Samples	100
GFDM Modulation Order	64
Number of Allocated Subcarriers	64
Transmitter Cyclic Prefix (CP)	8
Carrier Frequency	25GHz
Roll-Off Factor	0.5
Overlapping Subcarriers	2
Modulation Scheme	QAM
Total Concatenated GFDM Blocks	5
Filter Span in Symbols	10
Normalized SNR	40dB
Communication Channel	Rayleigh Channel
Length of GFDM Packets	10240
Number of Samples per Sub-Symbols	6

4.1. Comparative Analysis of the Proposed Method over Existing Studies

In this section, the performance achieved by the proposed method is analyzed using a graphical illustration of different metrics like BER, CCDF, PAPR, computation time, and convergence analysis. A detailed analysis of the graphical illustration is depicted below.

4.1.1. Comparative Analysis of BER Performance

The BER is the error measure within the given time interval and the ratio of error bits to the total inputted bits over the Improved Hippopotamus Optimization (ImHO)-GFDM system model.

$$BER = \frac{Amount\ \ of\ \ error\ \ samples}{Total\ \ inputted\ \ samples} \tag{21}$$

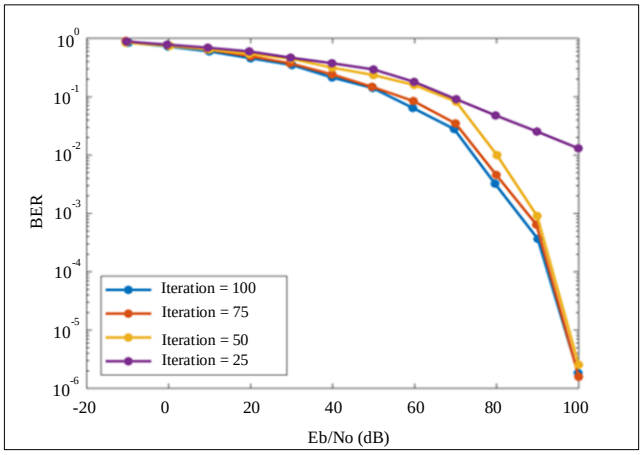

Fig. 2 BER analysis under roll-off factors

Figure 2 represents the BER analysis for various iterations of the ImHO algorithm. Here, the optimal best roll-off factor selection by the ImHO algorithm assists in enhancing the performance. The RO factors from the proposed squared cosine PSF are considered to minimize the noise without destroying useful information. From the graphical illustration, the BER reduces for higher iteration of the ImHO optimization algorithm.

The BER is analyzed for the proposed ImHO-GFDM system by varying the SNR. For iteration 25 and SNR of -5dB, the proposed system attains the BER of 0.88, which is 0.84 for 100 iterations. Thus, the higher number of iterations provides a better roll-off factor selection and assists in minimizing the BER.

Figures 3(a) and 3(b) depict the BER analysis across different channels and modulation schemes. The graphical data reveals that the Rayleigh channel effectively transmits signals to the receiver with minimal discrepancies. In contrast, the AWGN channel exhibits a higher error rate and potential data losses, making it less suitable for modern multicarrier communication systems. The proposed ImHO-GFDM system uses the Rayleigh channel for sending, transmitting, and receiving signals, demonstrating very low data losses and making it highly recommended for 5G applications.

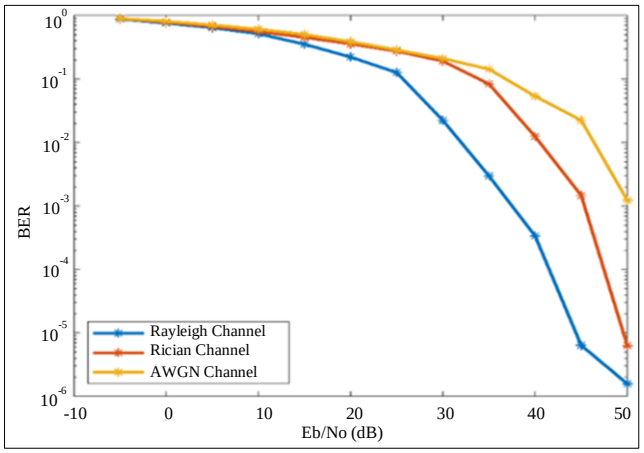

Fig. 3(a) BER analysis under varying channels

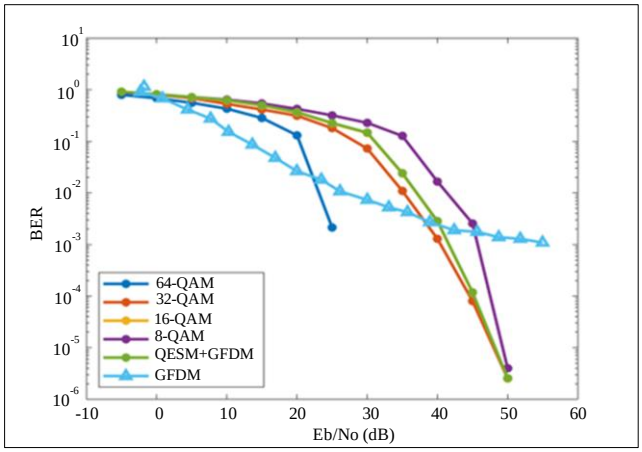

Fig. 3(b) BER analysis under varying modulations

4.1.2. Comparative Analysis over CCDF and PAPR Performance

The PAPR is defined as the ratio of the maximum power of the sample in the GFDM transmitting symbols to the average power of these GFDM symbols, and it can be mathematically formulated as follows.

$$PAPR_{dB}(z[m]) = 10\log_{10}\left(\frac{\max_{0\le m\le ML}|z[m]|^2}{E(|z[m]|^2)}\right) \quad (22)$$

Here, z[m] signifies the transmitting signal, MLrepresents the oversampling factor, max|.| indicates the maximum value and E(.) represents the statistical mean. The PAPR can be estimated accurately using the Complementary Cumulative Distribution Function (CCDF). Assuming the PAPR threshold as, $PAPR_0>0$, the probability $PAPR_{dB}$ is greater than the threshold obtained by the CCDF and it can be mathematically formulated as,

$$CCDF(PAPR_0) = P(PAPR_{dB} > PAPR_0) \quad (23)$$

Here, P represents the probability. For simulation, the RO factor of 0.1 and the subcarrier of 64 and 6 sub-symbols are considered.

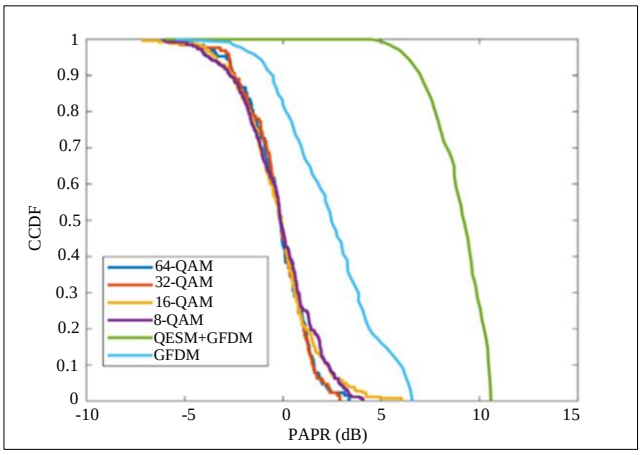

Fig. 4 CCDF versus PAPR analysis under varying modulations

Figure 4 shows the connection between CCDF and PAPR for different modulation schemes. The figure reveals that 64 QAM is particularly effective in modulating the GFDM signal, offering efficient performance. In contrast, 8 QAM and 16 QAM exhibit lower efficiency, leading to a degradation of the signal's useful information. A suitable modulation scheme is essential for enhancing the communication performance of large-scale systems. The proposed approach utilizes 64 QAM to modulate the GFDM signal, ensuring the integrity of the transmitted signal.

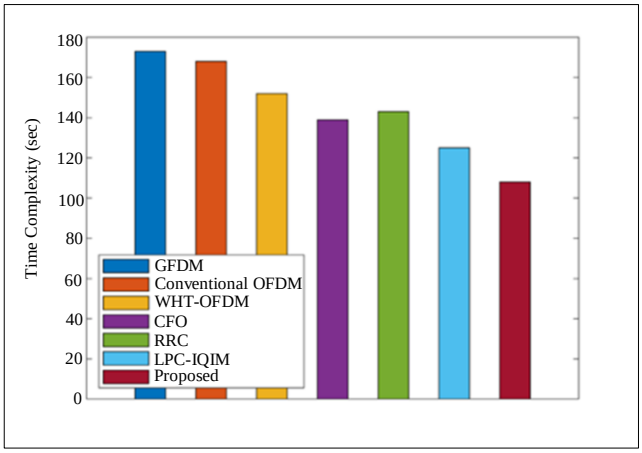

Fig. 5 Computation time

The computation complexity-based analysis is portrayed in Figure 5. The proposed ImHO -GFDM evaluated the time complexity of 110Sec, which is minimal compared to the existing methods. The convergence analysis of the proposed ImHO algorithm compared to the conventional HO algorithm is presented in Figure 6.

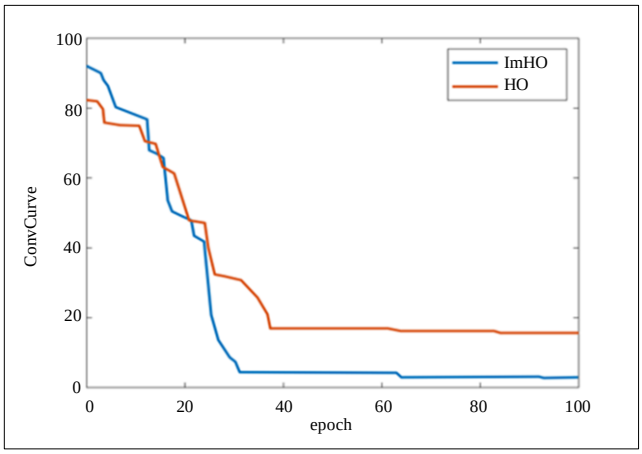

Fig. 6 Convergence analysis

Here, the analysis portrays the faster convergence of the proposed ImHO algorithm in pulse shaping due to the iterative chaotic mapping.

4.2. Comparative Discussion

A comparison of ImHO-GFDM with existing methods, such as CFO [22], RRC [25], and LPC-IQIM [21], underscores its advantages. ImHO-GFDM achieves lower BER than these methods by incorporating several innovative techniques to address the limitations of previous solutions. Unlike Kumar and Prasad's linear constellation precoded GFDM [21], which suffers from interference issues as the number of users grows, ImHO-GFDM combines spatial modulation and pulse shaping to improve diversity and effectively reduce interference.

Furthermore, unlike Wang et al.'s CFO [22] evaluation technique and music algorithm, which experience performance degradation in advanced 5G applications, ImHO-GFDM provides reliable carrier frequency offset estimation and noise resistance through its integrated pulse shaping and modulation strategies. Moreover, unlike Gupta and Gamad's root-raised cosine filtering method [25], which lacks flexibility and leads to increased data losses in modern 5G systems, ImHO-GFDM offers greater adaptability and efficiency through its holistic design, resulting in superior BER performance and making it well-suited for emerging wireless communication standards.

4.2.1. Practical Implications

ImHo-GFDM has significant practical implications for wireless communications, offering a comprehensive solution to enhance the efficiency, reliability, and performance of next-generation networks, especially 5G and beyond. Its ability to reduce interference, improve diversity, and provide robust carrier frequency offset estimation makes it well-suited to meet the increasing demand for high-speed data transmission, low-latency communication, and reliable connectivity across various deployment scenarios. Additionally, its adaptability and flexibility ensure its relevance in evolving standards and emerging technologies, making it a valuable solution in the rapidly changing landscape of modern wireless communication systems.

5. Conclusion

This study introduces a new ImHo-GFDM approach for 5G and beyond GFDM systems, utilizing an innovative pulse shape filtering scheme to eliminate interference within the GFDM signal effectively. The proposed modulation scheme significantly reduces PAPR and CCDF while maximizing data rates for multicarrier users. It demonstrated strong performance in recovering the original transmitted signal at the receiver. Computer simulations using MATLAB were conducted to evaluate key metrics such as BER, PAPR, computation time, convergence analysis and CCDF, showing that the method achieved an overall BER at a 1.58×10^{-6} 50dB SNR. However, the current study does not analyze the resulting waveforms for embedded services or multicarrier communication systems, limiting its practical applicability.

Future work will extend this study by incorporating GFDM waveforms within MIMO systems alongside a channel estimation process to analyze BER performance better. While the method shows promising results regarding BER, PAPR, and CCDF, its limitations present opportunities for further research. Specifically, the absence of analysis for embedded services and multicarrier communication systems is a gap that can be addressed in future work. Expanding the research to include support for such systems and extending the scope to MIMO channels will enhance the method's relevance and effectiveness for practical wireless communication applications.

References

[1] Surbhi Kalsotra, Ashutosh Kumar Singh, and Hem Dutt Joshi, "Performance Analysis of Space Time Coded Generalized Frequency Division Multiplexing System over Generalized Fading Channels," *Transactions on Emerging Telecommunications Technologies*, vol. 33, no. 4, 2022. [CrossRef] [Google Scholar] [Publisher Link]

[2] Guilherme P. Aquino, and Luciano L. Mendes, "Sparse Code Multiple Access on the Generalized Frequency Division Multiplexing," *EURASIP Journal on Wireless Communications and Networking*, vol. 2020, 2020. [CrossRef] [Google Scholar] [Publisher Link]

[3] Muhammad Sameer Ahmed, and Tansal Gucluoglu, "Performance of Generalized Frequency Division Multiplexing over Gamma Gamma Free Space Optical Link," *Optics Communications*, vol. 466, 2020. [CrossRef] [Google Scholar] [Publisher Link]

[4] S. Chitra et al., "Performance Enhancement of Generalized Frequency Division Multiplexing with RF Impairments Compensation for Efficient 5G Wireless Access," *AEU-International Journal of Electronics and Communications*, vol. 127, 2020. [CrossRef] [Google Scholar] [Publisher Link]

[5] Rajath P. Hebbar, and Prerana Gupta Poddar, "Generalized Frequency Division Multiplexing–Based Acoustic Communication for Underwater Systems," *International Journal of Communication Systems*, vol. 33, no. 10, 2020. [CrossRef] [Google Scholar] [Publisher Link]

[6] Ching-Lun Tai, Tzu-Han Wang, and Yu-Hua Huang, "An Overview of Generalized Frequency Division Multiplexing (GFDM)," *arXiv*, 2020. [CrossRef] [Google Scholar] [Publisher Link]

[7] Muhammad Sameer Ahmed, and Tansal Gucluoglu, "Maximum Ratio Transmission Based Generalized Frequency Division Multiplexing over Gamma-Gamma Channel," *Optics Communications*, vol. 492, 2021. [CrossRef] [Google Scholar] [Publisher Link]

[8] Ersin Öztürk, Ertugrul Basar, and Hakan Ali Çırpan, "Multiple-Input Multiple-Output Generalized Frequency Division Multiplexing with Index Modulation," *Physical Communication*, vol. 34, pp. 27-37, 2019. [CrossRef] [Google Scholar] [Publisher Link]

[9] T. Perarasi et al., "Evaluation of Cooperative Spectrum Sensing with Filtered Bank Multi Carrier Utilized for Detecting in Cognitive Radio Network," *Transactions on Emerging Telecommunications Technologies*, vol. 33, no. 7, 2022. [CrossRef] [Google Scholar] [Publisher Link]

[10] Mohammad Hussein Amiri et al., "Hippopotamus Optimization Algorithm: A Novel Nature-Inspired Optimization Algorithm," *Scientific Reports*, 2024. [CrossRef] [Google Scholar] [Publisher Link]

[11] Ahmad Nimr et al., "Generalized Frequency Division Multiplexing: Unified Multicarrier Framework," *Radio Access Network Slicing and Virtualization for 5G Vertical Industries*, 2020. [CrossRef] [Google Scholar] [Publisher Link]

[12] Eslam Mansour Shalaby, Saleh Ibrahim Hussin, and Moawad Ibrahim Dessoky, "Performance Evaluation of 5G Modulation Techniques," *Wireless Personal Communications*, vol. 121, pp. 2461-2476, 2021. [CrossRef] [Google Scholar] [Publisher Link]

[13] Ravi Sekhar Yarrabothu et al., "SER Analysis of Generalized Frequency Division Multiplexing under Various Real Time Fading Conditions," *International Journal of Control Theory and Applications*, vol. 10, no. 21, pp. 151-158, 2017. [Google Scholar] [Publisher Link]

[14] R. Anil Kumar, and K. Satya Prasad, "Performance Analysis of GFDM Modulation in Heterogeneous Network for 5G NR," *Wireless Personal Communications*, vol. 116, pp. 2299-2319, 2021. [CrossRef] [Google Scholar] [Publisher Link]

[15] Mozaffari Tazehkand Behzad et al., "Optimal Prototype Filter Design Based on New Mathematical Model of GFDM System," *arXiv*, 2023. [CrossRef] [Google Scholar] [Publisher Link]

[16] Ajib Setyo Arifin, "Study and Experiment of Generalized Frequency Division Multiplexing Implementation Using USRP and LabVIEW," *International Conference on Computer Science and Its Application in Agriculture (ICOSICA)*, pp. 1-5, 2020. [CrossRef] [Google Scholar] [Publisher Link]

[17] Muhammad Sameer Ahmed, Piotr Remlein, and Tansal Gucluoglu, "Impact of Weather Conditions on Generalized Frequency Division Multiplexing over Gamma Gamma Channel," *International Journal of Information and Communication Engineering*, vol. 14, no. 11, pp. 376-379, 2020. [Google Scholar] [Publisher Link]

[18] Jannatul Ferdows et al., "Symbol Error Rate Calculation for Generalized Frequency Division Multiplexing in 5G Wireless Communication Systems," *International Research Journal of Advanced Engineering and Science*, vol. 3, no. 4, pp. 97-99, 2018. [Google Scholar] [Publisher Link]

[19] Yung-Yi Wang, and Shih-Jen Yang, "Estimation of Carrier Frequency Offset and Channel State Information of Generalize Frequency Division Multiplexing Systems by Using a Zadoff–Chu Sequence," *Journal of the Franklin Institute*, vol. 359, no. 1, pp. 637-652, 2022. [CrossRef] [Google Scholar] [Publisher Link]

[20] Sai Sahitya Kasa et al., "Performance Analysis of Generalized Frequency Division Multiplexing in Cognitive Radio under Fading Channels," *TEQIP III Sponsored International Conference on Microwave Integrated Circuits, Photonics and Wireless Networks (IMICPW)*, Tiruchirappalli, India, pp. 387-392, 2019. [CrossRef] [Google Scholar] [Publisher Link]

[21] Relangi Anil Kumar, and K. Satya Prasad, "Performance Analysis of an Efficient Linear Constellation Precoded Generalized Frequency Division Multiplexing with Index Modulation in 5G Heterogeneous Wireless Network," *International Journal of Communication Systems*, vol. 34, no. 4, 2021. [CrossRef] [Google Scholar] [Publisher Link]

[22] Yung-Yi Wang, Shih-Jen Yang, and Ting-Chieh Lin, "Efficient Carrier Frequency Offset Estimation Algorithm for Generalized Frequency Division Multiplexing Systems," *Signal Processing*, vol. 172, 2020. [CrossRef] [Google Scholar] [Publisher Link]

[23] Pawan Kumar et al., "Impact of Peak to Average Power Ratio Reduction Techniques on Generalized Frequency Division Multiplexing for 5th Generation Systems," *Computers and Electrical Engineering*, vol. 95, 2021. [CrossRef] [Google Scholar] [Publisher Link]

[24] Imran A. Tasadduq, "CPM-GFDM: A Novel Combination of Continuous Phase Modulation and Generalized Frequency Division Multiplexing for Wireless Communication," *Applied Sciences*, vol. 13, no. 2, 2023. [CrossRef] [Google Scholar] [Publisher Link]

[25] Megha Gupta, and R.S. Gamad, "Symbol Error Rate Analysis of Generalized Frequency Division Multiplexing in Pulse Shaping Root Raised Cosine Filter," *IEEE 11th International Conference on Communication Systems and Network Technologies (CSNT)*, Indore, India, pp. 647-650, 2022. [CrossRef] [Google Scholar] [Publisher Link]

[26] Ali Asghar Heidari et al., "Harris Hawks Optimization: Algorithm and Applications," *Future Generation Computer Systems*, vol. 97, pp. 849-872, 2019. [CrossRef] [Google Scholar] [Publisher Link]

[27] Weiguo Zhao, Liying Wang, and Zhenxing Zhang, "Artificial Ecosystem-Based Optimization: A Novel Nature-Inspired Meta-Heuristic Algorithm," *Neural Computing and Applications*, vol. 32, pp. 9383-9425, 2020. [CrossRef] [Google Scholar] [Publisher Link]

[28] Benyamin Abdollahzadeh, Farhad Soleimanian Gharehchopogh, and Seyedali Mirjalili, "African Vultures Optimization Algorithm: A New Nature-Inspired Metaheuristic Algorithm for Global Optimization Problems," *Computers & Industrial Engineering*, vol. 158, 2021. [CrossRef] [Google Scholar] [Publisher Link]